

An Extensionally Fractured Upper Lithosphere on Io

Paul K. Byrne^{1*}, Rosaly M. C. Lopes², Jani Radebaugh³, and David A. Williams⁴

¹Washington University in St. Louis, St. Louis, MO 63130, USA.

²Jet Propulsion Laboratory, California Institute of Technology, Pasadena, CA 91109, USA.

³Brigham Young University, Provo, UT 84602, USA.

⁴Arizona State University, Tempe, AZ 85287, USA.

*Corresponding author: Paul Byrne (paul.byrne@wustl.edu)

Key Points:

- A distinctive polygonal “island” in Io’s largest patera may be a fractured crustal block
- There are numerous other indicators for a pervasively fractured Ionian lithosphere
- We propose a lithospheric model for Io with major shortening and extensional tectonics in the lower and upper portions, respectively

25 **Abstract**

26 The Jovian moon Io features hundreds of paterae, broad depressions often filled with lava. The largest
 27 such example, Loki Patera, features a large, polygonal, and fractured island in its center. This island
 28 may reflect the fragmentation of the upper Ionian lithosphere by a shallow magma body, facilitated by
 29 a great number of shallow extensional structures. We propose a model for the Ionian lithosphere in
 30 which the upper portion is heavily deformed by joints, normal faults, and graben resulting from
 31 combined tidal, subsidence, and thermal stresses, and a lower portion rife with major thrust faults
 32 formed by horizontal compression of deeper crustal levels from the continued burial of surface units.
 33 Some of those thrusts may be reactivated normal faults. An extensionally fractured upper lithosphere
 34 accounts for the Loki Patera island, for observations of more than 175 paterae with straight edges, for
 35 the fact that almost 95% of Io's surface is covered with volcanic flow and plains units, and for
 36 widespread instances of mass wasting within Io's gigantic mountain blocks. Additional, high-resolution
 37 image and topographic data are required to test this hypothesized model for the moon's lithosphere.

38

39 **Plain Language Summary**

40 Io is a large moon of Jupiter, and one of the most volcanically active bodies in the Solar System. Io has
 41 a distinctive landform type called “paterae” (“patera” in singular form), which are essentially large
 42 depressions filled with lava. The biggest patera is called Loki Patera, and in its middle is a polygonal
 43 island. We interpret this island as a fractured block of Io's crust. If this interpretation is correct, then it
 44 is possible that much of the upper portion of Io's crust is riddled with extensional fractures caused by
 45 several overlapping processes. A huge number of extensional fractures explains other aspects of Io's
 46 geology, such as the fact that almost half of all the moon's paterae have straight edges—which is
 47 something we'd expect to happen if paterae form in a heavily extensionally fractured crust. Io also has
 48 gigantic mountains, which are formed by compression of the lower crust as tremendous amounts of

lava erupt and bury everything around them. But even those mountains show lots of extensional tectonic structures, which provide further support for our idea about Io's crust.

1 Introduction

Jupiter's rocky moon Io is replete with towering mountain blocks (Schenk et al., 2001) and lava flows that cover virtually the entire surface (McEwen et al., 1998; Williams et al., 2011). Internal heat energy is principally supplied by tidal interactions with Jupiter and its neighboring moons (Peale et al., 1979). Chief among the satellite's most notable landforms are the paterae, broad depressions that are widespread and commonly filled with lavas (Radebaugh et al., 2001).

First described by Carr et al. (1979), paterae (*sing.* patera) are quasi-circular, shallow depressions with curved, straight, or scalloped edges. These landforms may be the Ionian equivalent to the calderas seen on Earth, Venus, and Mars, but a formation via collapse into a subsurface void space—the principal means by which calderas form (Lipman, 1997)—has yet to be confirmed for Io's paterae. Radebaugh et al. (2001) identified at least 417 paterae (425 including nested features: Williams et al., 2011) distributed across the ~80% of Io imaged at 2 km/pixel or better, with diameters ranging from 2.5 to 202.6 km.

That largest patera is Loki, situated in Io's eastern hemisphere. Loki Patera features a prominent "island" in its center (Lopes-Gautier et al., 2000). Dark lines that cross this island are suggestive of tectonic lineaments—raising the possibility that the island is a fractured crustal block. If so, then the break-up of this block may offer valuable insights into the properties and tectonic state of Io's lithosphere.

2 The Loki Patera Island

Seen with combined data from the Voyager 1 Imaging Science Subsystem narrow-angle camera and the Galileo Solid-State Imaging System (SSI) camera (Figure 1a), the island is distinctly polygonal in

outline and measures approximately 115×110 km in spatial extent along its north–south and east–west axes, respectively. A prominent lineament about 85 km long strikes east–northeast across the island, with two additional linear features (55 and 30 km long, respectively) striking to the northeast and abutting the first. Each of these features is $\sim 2\text{--}3$ km across. Smaller polygonal “islands” are present to the northwest and southwest of the larger block, and the dark patera floor is dotted with bright spots (termed “bergs”) that may be locally high-standing topography and/or surface deposits (Howell et al., 2013).

The morphology of these lineaments strongly suggests that they are extensional tectonic structures. Although lava flows can be much longer than they are wide, they tend to show digitate ends and widen with distance from their source vents (e.g., Carr et al., 1977) and so are not morphologically consistent with the Loki Patera island lineaments. Neither are other geological landforms that can have relatively linear planforms, such as mass-wasting deposits nor secondary crater chains (of which no examples are yet known for Io). Dikes often have straight margins that extend for tens of kilometers or more, but on that scale are bounded by steep, near-vertical fractures (e.g., Ernst et al., 2001). We therefore interpret these lineaments as being extensional in nature, either tensile fractures (i.e., joints) or, more likely given their scale, are paired, antithetic, inward-dipping normal faults (i.e., graben).

Near-Infrared Mapping Spectrometer data returned by the Galileo mission indicate that both the patera floor and the material within these fractures are warmer than the island and the plains surrounding the patera (Lopes-Gautier et al., 2000); these thermal characteristics are shared by many other paterae on Io (Radebaugh et al., 2001). Per our reasoning, the Loki Patera island is in fact several discrete (but formerly contiguous) blocks that have rafted apart in a manner akin to pack ice, and the material between the blocks is the lava that covers the entire patera floor. Comparison of image data of Loki Patera from the Galileo and Voyager missions indicate that the island and its constituent fractures show no resolvable change in position or size over the intervening two decades (Lopes-Gautier et al., 2000). Moreover, the kinetic and thermal effects of two concurrent resurfacing “waves” observed in

March 2015 did not appear to disrupt or destroy the island, strongly indicating that this feature has persisted for at least the 36 years since its discovery in 1979, and that it may now be sitting on, or is anchored to, the patera floor (de Kleer et al., 2017).

3 Implications for Ionian Volcanotectonics

3.1 Patera Formation

As large, irregular depressions overwhelmingly associated with lava flows, paterae have been interpreted as the Ionian counterparts to calderas on Earth, Venus, and Mars (e.g., Carr et al., 1979). Yet calderas on those worlds are generally characterized by quasi-circular or arcuate outlines (Crumpler et al., 1996) and peripheral zones of crustal extension (Walter and Troll, 2011), and are frequently associated with voluminous deposits of lava, ash, or both (Lipman, 1997). Indeed, 42% of the 417 paterae surveyed by Radebaugh et al. (2001) have straight or irregular margins that terminate at sharp corners (e.g., Figure 2). Adjacent extensional structures are not commonly observed, although this dearth of extensional tectonics may be a function of available image resolution and Io's prodigious global resurfacing rate of ~1.5 cm/yr (Kirchoff and McKinnon, 2009). And no volcanic deposits of sufficient volume to match the observed depression have been unequivocally recognized proximal to, and having come from, any patera (Keszthelyi et al., 2004).

Paterae may instead be the result of the stalling of silicate magma at shallow depths that undermines the overlying crust, particularly if that crust is SO₂ rich and porous (Keszthelyi et al., 2004). Under this scenario, the heat from an intrusion melts sulfur and/or SO₂, which mobilizes into the surrounding country rock and leaves behind pore space. With continued melting, a substantial depression forms or the magma chamber can even be fully unroofed (Keszthelyi et al., 2004). By this view, Io's paterae differ from conventional calderas by forming not because of the eruption or lateral withdrawal of magma but by the migration of volatiles through a crust that becomes increasingly porous or otherwise mechanically weak (cf. Kargel et al., 1999).

Regardless of the means of collapse, the disruption of a magma chamber roof would be readily enhanced by pre-existing extensional fractures in the crust—such as those that cross the Loki Patera island. We infer that these structures predate the formation of Loki Patera for two reasons: a) they do not have a spatial distribution or arrangement consistent with extensional strains associated with magma chamber tumescence or collapse (e.g., Walter and Troll, 2001); and b) at tens of km long, their dimensions are comparable to the lengths of those portions of other paterae margins that are straight and have been interpreted to reflect tectonic control (e.g., Radebaugh et al., 2001).

It may be, then, that the island is a remnant of fractured crust that overlaid and foundered into a shallow, stalled magma body. The rest of the roof material might even have been subsumed by lava entirely, accounting for why there are few similar, fractured islands in other paterae. (Some other paterae have islands, such as the 28 km-diameter Steropes Patera (Radebaugh et al., 2001) or the 75 km-wide Tupan Patera (Black, 2006), but available image data are insufficient to survey all such examples on Io, or determine how many, if any, are also fractured.) Further, should the Loki block be sitting on the patera floor, sufficiently anchored so as to remain seemingly stationary at least since its first observation in 1979 (de Kleer et al., 2017), then it follows that as a result of the creation of void space in the subsurface, the block's upper surface should be lower than the surrounding plains. Lava from floor eruptions could then exploit and undermine fractures in the island to thermally erode and enlarge them, such that those structures become visible at Voyager image resolutions.

3.2 *Fracturing of the Ionian Upper Lithosphere*

The fractured block in Loki, the finding of almost half of all paterae having straight margins, and the fact that some patera walls are steep and stand kilometers tall—such as the margins of Chaac Patera, which are 2.7 km high and have slopes of 70° (Radebaugh et al., 2001)—together imply strong tectonic control on the formation of at least some paterae. Certainly *thrust* faults are widespread on Io, with the straight margins of many of the moon's enormous mountain blocks (Figure 3) taken as evidence of

shortening tectonics, attributed to subsidence of the crust under continually emplaced lavas (Schenk and Bulmer, 1998; Turtle et al., 2001).

But there are reasons to expect substantial *extensional* deformation of the upper Ionian lithosphere, too. For example, temporally and spatially localized decreases in eruptive activity, set against a backdrop of sustained tidal heating, are predicted to generate considerably large, horizontally compressive stresses deep in the Ionian crust, but horizontally extensional stresses near the surface (McKinnon et al., 2001; Kirchoff et al., 2020). Similarly, the formation of Io's gigantic mountain blocks along deep-seated thrust faults is thought to be accompanied by widespread extension and the formation of normal faults and graben (Bland and McKinnon, 2016). Some of these extensional structures may penetrate as much as 15 km into the footwall (Bland and McKinnon, 2016)—consistent with the great heights and slope angles of, for instance, the Chaac Patera walls. Extensional fractures would efficiently conduct ascending magma to the surface (Bland and McKinnon, 2016; McGovern et al., 2016; Byrne et al., 2018), allowing magma to erupt that would otherwise be too dense to avoid stalling in the shallow crust (Keszthelyi et al., 2004). At least some of these extensional structures have a dip component of slip (Ahern et al., 2017).

Even within the uplifted and tilted mountain blocks, there is considerable extensional deformation, such as the scarp-parallel lineaments on the back scarps of the Hi'iaka Montes (Ahern et al., 2017) (Figure 3). Similarly, Schenk and Bulmer (1998) documented landslide scarps on Euboea Montes—presumably great listric normal faults, on the basis of comparisons with landslide deposits on Earth and other planets (e.g., Lopes et al., 1980; Riley et al., 1999).

4 Discussion

A highly extensionally deformed upper, brittle lithosphere accounts for several separate but related sets of observations of Io.

173 Firstly, the prevalence of such structures explains why the central island in Loki Patera has a
 174 polygonal outline and appears dissected by fractures: the island is a formerly coherent block that broke
 175 apart along pre-existing fractures atop a shallow magma body as that body (and the patera) grew, by the
 176 withdrawal and/or eruption of magma, via the mobilization of sulfur-bearing volatiles (Keszthelyi et
 177 al., 2004), or by a combination of these processes. In any case, since *some* subsurface material was
 178 removed, that central island must now be at a lower elevation than the surrounding plains and is
 179 perhaps sitting on the patera floor. The smaller islands and bergs in Loki may be other, smaller
 180 fragments of the original chamber roof, consistent with the view of Howell et al. (2013) that such
 181 features are not concentrations of sulfur deposits but are instead isolated areas of terrain that avoided
 182 burial by subsequent lavas. It is not clear why the large island has remained intact, in contrast to some
 183 of the smaller fragments throughout the patera floor (Howell et al., 2013), although there may well be a
 184 resolution effect at play since those smaller fragments visible in Voyager images are not resolved with
 185 Galileo data. The island may simply be the largest remaining piece of an ongoing process that will
 186 ultimately destroy the original roof over the magma body entirely, in which case Loki will eventually
 187 come to resemble other paterae where no large islands are present—and, by implication, other paterae
 188 may once have had large island fragments.

189 Secondly, widespread joints and normal faults in the crust account for the straight margins of a
 190 substantial number of Io's paterae (Radebaugh et al., 2001), with these structures forming the
 191 boundary(ies) of patera(e) as shallow magma bodies undermined and drove the collapse of the
 192 overlying, fractured roof material (Keszthelyi et al, 2004). The numerous instances of sharp paterae
 193 corners noted by Radebaugh et al. (2001) might reflect the tectonic influence of intersecting sets of
 194 joints or normal faults. Moreover, the extension associated with the mountain formation models of
 195 Bland and McKinnon (2016) and Kirchoff et al. (2020) is consistent with the finding that paterae—
 196 assuming their form is controlled by pre-existing normal faults—are much more commonly collocated
 197 with mountains than predicted by chance alone (Radebaugh et al. 2001; Jaeger et al., 2003).

Thirdly, abundant extensional structures provide ready conduits for magma to reach the surface; indeed, the normal and transtensional fractures that characterize an extensional tectonic regime are more conducive to magma ascent than reverse or transpressional fractures, given that crustal shortening results in negative horizontal elongation whereas horizontal extension opens vertical accommodation space into which magma can move (e.g., Byrne et al., 2018). A prevailing horizontally extensional tectonic regime in its upper lithosphere is thus compatible with Io being almost entirely covered by extensive lava flows and vast plains units, the latter of which mainly comprise buried lavas and pyroclastic deposits (McEwan et al., 2000; Williams et al., 2002). Indeed, plains and lava flow units occupy 66.6% and 27.8% of the surface, respectively (Williams et al., 2011).

Finally, Schenk and Bulmer (1998) proposed that uplifted blocks rise along deep-rooted thrust faults, drawing a parallel between Io's mountains and basement-cored uplifts in the western United States. In the latter case, those shortening structures moved along reactivated, high-angle normal faults that originally formed via crustal extension (e.g., Reches, 1978). For horizontal compression, incipient thrust faults form with low dip angles (Anderson, 1905). Therefore, should at least some mountain blocks be bounded by high-angle reverse faults as suggested by Ahern et al. (2017), then those bounding structures could have formed as normal faults that were later reactivated when horizontally compressive stresses built at the base of the lithosphere from sustained burial of surface materials (Bland and McKinnon, 2016).

We thus propose a model for Io whereby the upper lithosphere features a pervasive fracture network formed by a combination of tidal, subsidence, and thermal stresses—with large, deep-seated thrust faults and widespread normal faults dominant at lower and upper crustal levels, respectively (Figure 4). Abundant extensional structures at shallow crustal levels serve as failure planes along which undermined magma chamber roofs collapse, and are available for reactivation with a reverse or oblique sense of slip if favorably aligned to local, subsequent stress fields. The apparent dearth of extensional strain (beyond paterae and mountain block edges) on Io is probably a function of the moon's

extraordinary volcanic resurfacing rate, which likely obscures just how deformed the near surface actually is.

This stress state is in marked contrast to other terrestrial bodies in the Solar System. For instance, although there are major thrust fault-related landforms on Mercury as is the case on Io, those on the innermost planet are interpreted to have formed from secular interior cooling (Strom et al., 1975; Byrne et al., 2018). The resulting horizontally compressive stress field results in a dearth of extensional structures at the surface, and inhibits the ascent of magma to shallow depths in all but the weakest parts of the planet's crust (Byrne et al., 2018). The tectonic characteristics of Mercury are largely shared by the Moon (e.g., Byrne, 2020). Venus and Earth are replete with both extensional and shortening landforms, although each is in a different tectonic regime than that of Io (e.g., Byrne, 2020; Lourenço et al. 2020). Mars, too, has widespread extensional tectonics (e.g., Byrne, 2020), attributed at least in part to near-surface stresses associated with the Tharsis Rise (e.g., Anderson et al., 2001), as well as shortening structures reflecting both Tharsis-related loading stresses and global contraction (e.g., Nahm and Schultz, 2010). But none of the inner Solar System worlds has a tectonic inventory matching Io.

The Jovian moon is also distinctive among outer Solar System satellites in that it is the only such body without an icy exterior. Although tectonic structures including graben and thrust fault-related landforms are widespread on myriad other icy moons (e.g., Collins et al., 2010), none boasts the elevated mountain blocks nor visibly craterless surface of Io (Williams et al., 2011). Io's tectonic stress state is the result principally of its inordinate effusive volcanism, which in turn is driven by the dissipation of tidal energy in its interior (Peale et al., 1979). By this measure, Io's lithospheric stress state may be unique in the Solar System—but could be illustrative of tidally heated planets orbiting other stars (Barr et al., 2018; McEwen et al., 2020).

5 Conclusions

The distinctive, polygonal “island” in Loki Patera holds clues to Io’s lithospheric stress state. This island may be a fractured crustal block, the remains of a portion of the crust undermined by a shallow magma body aided by widespread extensional deformation. A heavily extensionally deformed upper lithosphere, likely by a combination of subsidence, tidal, and thermal stresses, accounts for several seemingly disparate observations, including:

- 1) The polygonal, fractured appearance of the Loki Patera island;
- 2) A substantial number of other paterae with straight edges;
- 3) A globally youthful surface; and
- 4) The extensional strains so commonly seen within Io’s enormous, uplifted mountains.

We therefore propose a scenario for Io under which the lower lithosphere is deformed by large, deep-seated thrust faults from the burial of surface materials, but that is also riven by extensional tectonics in the near surface.

The acquisition of image and topographic data at resolutions substantially greater than those returned by the Voyager and Galileo missions would enable the search for and measurements of joints, normal faults, and graben in the plains proximal to paterae and mountain blocks, and would also establish if the elevation of the upper surface of the island is in fact below that of the surrounding plains. Such data would also provide a valuable comparison for assessing whether the Loki island really has remained stationary since its discovery. Further, the detection of small-scale extensional structures undergoing burial by active volcanism would lend support to the hypothesis that the Ionian lithosphere is far more tectonically disrupted than previously recognized.

Open Research

No new data were created for this study. All Voyager and Galileo image data used in this paper are publicly available at the NASA Planetary Data System (PDS) at <https://pds.nasa.gov>. The photogeological data shown in Fig. 1a and used for preparing the structural sketch in Fig. 1b (and for

the surface texture of the block in Fig. 4) is the combined Voyager–Galileo SSI global 1 km/px mosaic, available at https://astrogeology.usgs.gov/search/map/Io/Voyager-Galileo/Io_GalileoSSI-Voyager_Global_Mosaic_1km. The data used to generate Figs. 2 and 3 are from the Galileo Solid-State Imaging (SSI) dataset (Thaller, 2000).

Acknowledgments

Part of this research was conducted at the Jet Propulsion Laboratory, California Institute of Technology, under contract with NASA. This research made use of NASA’s PDS and Astrophysics Data System.

References

- Ahern, A. A., Radebaugh, J., Christensen, E. H., Harris, R. A., & Tass, E. S. (2017), Lineations and structural mapping of Io’s paterae and mountains: Implications for internal stresses. *Icarus*, 297, 14–32. doi:10.1016/j.icarus.2017.06.004.
- Anderson, E. M. (1905), The dynamics of faulting. *Transactions of the Edinburgh Geological Society*, 8(3), 387–402. doi:10.1144/transed.8.3.387.
- Anderson, R. C., et al. (2001), Primary centers and secondary concentrations of tectonic activity through time in the western hemisphere of Mars. *Journal of Geophysical Research*, 106, 20563–20585. doi:10.1029/2000JE001278.
- Barr, A. C., Dobos, V., & Kiss, L. L. (2018), Interior structures and tidal heating in the TRAPPIST-1 planets. *Astronomy and Astrophysics*, 613, A37. doi:10.1051/0004-6361/201731992.
- Black, S. R. (2006). *The origin and evolution of islands in Ionian paterae* (Master’s thesis). Retrieved from UMI ProQuest Digital Dissertations. (1436720). New York: State University of New York at Buffalo.

- 296 Bland, M. T., & McKinnon, W. B. (2016), Mountain building on Io driven by deep faulting. *Nature*
297 *Geoscience*, 9, 429–433. doi:10.1038/NGEO2711.
- 298 Byrne, P. K, Whitten, J. L., Klimczak, C., McCubbin, F. M., & Ostrach, L. R. (2018), The volcanic
299 character of Mercury. In Solomon, S. C., Nittler, L. R., and Anderson, B. J. (eds.), Mercury: The
300 View after MESSENGER, 287–323. Cambridge University Press, Cambridge, UK.
301 doi:10.1017/9781316650684.012.
- 302 Byrne, P. K. (2020) A comparison of inner Solar System volcanism. *Nature Astronomy*, 4, 321–327.
303 doi:10.1038/s41550-019-0944-3.
- 304 Carr, M. H., Greeley, R., Blasius, K. R., Guest, J. E., & Murray, J. B. (1977), Some Martian volcanic
305 features as viewed from the Viking Orbiters. *Journal of Geophysical Research*, 82, 3985–4015.
306 doi:10.1029/JS082i028p03985.
- 307 Carr, M. H., Masursky, H., Strom, R. G., & Terrile, R. J. (1979), Volcanic features of Io. *Nature*, 280,
308 729–733. doi:10.1038/280729a0.
- 309 Collins, G. C., et al. (2010), Tectonics of the outer planet satellites. In Watters, T. R., and Schultz, R.
310 A. (eds.), Planetary Tectonics, Cambridge University Press, 264–350.
- 311 Crumpler, L. S., Head, J. W., & Aubele, J. C. (1996), Calderas on Mars: characteristics, structure, and
312 associated flank deformation. In McGuire, W. J., Jones, A. P., and Neuberg, J. (eds.), Volcano
313 Instability on the Earth and Other Planets, Geological Society Special Publication No. 110, 307–
314 348.
- 315 de Kleer, K., Skrutskie, M., Leisenring, J., Davies, A. G., Conrad, A., de Pater, I., Resnick, A., Bailey,
316 V., Defrère, D., Hinz, P., Skemer, A., Spalding, E., Vaz, A., Veillet, C., & Woodward, C. E. (2017),
317 Multi-phase volcanic resurfacing at Loki. *Nature*, 545, 199–202. doi:10.1038/nature22339.
- 318 Ernst, R. E., Grosfils, E. B., & Mège, D. (2001), Giant dike swarms: Earth, Venus, and Mars. *Annual*
319 *Review of Earth and Planetary Science*, 29, 489–534. doi:10.1146/annurev.earth.29.1.489.

- 320 Howell, R. R., Landis, C. E., & Lopes, R. M. C. (2013), Composition and location of volatiles at Loki
- 321 Patera, Io. *Icarus*, 229, 328–339. doi:10.1016/j.icarus.2013.11.016.
- 322 Jaeger, W. L., Turtle, E. P., Keszthelyi, L. P., Radebaugh, J., & McEwan, A. S. (2003), Orogenic
- 323 tectonism on Io. *Journal of Geophysical Research*, 108, E8, 5093. doi:10.1029/2002JE001946.
- 324 Kargel, J. S., Delmelle, P., & Nash, D. B. (1999), Volcanogenic sulfur on Earth and Io: Composition
- 325 and spectroscopy. *Icarus*, 142, 249–280. doi:10.1006/icar.1999.6183.
- 326 Keszthelyi, L., Jaeger, W. L., Turtle, E. P., Milazzo, M., & Radebaugh, J. (2004), A post-Galileo view
- 327 of Io’s interior. *Icarus*, 169, 271–286. doi:10.1016/j.icarus.2004.01.005.
- 328 Kirchoff, M. R., & McKinnon, W. B. (2009), Formation of mountains on Io: Variable volcanism and
- 329 thermal stresses. *Icarus*, 201, 598–614. doi:10.1016/j.icarus.2009.02.006.
- 330 Kirchoff, M. R., McKinnon, W. B., & Bland, M. T. (2020), Effects of faulting on crustal stresses
- 331 during mountain formation on Io. *Icarus*, 335, 113326. doi:10.1016/j.icarus.2019.05.028.
- 332 Lipman, P. W. (1997), Subsidence of ash-flow calderas; relation to caldera size and magma-chamber
- 333 geometry. *Bulletin of Volcanology*, 59, 198–218. doi:10.1007/s004450050186.
- 334 Lopes, R. M. C., Guest, J. E., & Wilson, C. J. (1980), Origin of the Olympus Mons aureole and
- 335 perimeter scarp. *The Moon and Planets*, 22, 221–234. doi:10.1007/BF00898433.
- 336 Lopes-Gautier, R. M. C., Douté, S., Smythe, W. D., Kamp, L. W., Carlson, R. W., Davies, A. G.,
- 337 Leader, F. E., McEwan, A. S., Geissler, P. E., Kieffer, S. W., Keszthelyi, L., Barbinis, E., Mehlman,
- 338 R., Segura, M., Shirley, J., & Soderblom, L. A. (2000), A close-up look at Io from Galileo’s near-
- 339 infrared mapping spectrometer. *Science*, 288, 1201–1204. doi:10.1126/science.288.5469.1201.
- 340 Lourenço, D. L., Rozel, A. B., Ballmer, M. D., & Tackley, P. J. (2020), Plutonic-squishy lid: A new
- 341 global tectonic regime generated by intrusive magmatism on Earth-like planets. *Geochemistry,*
- 342 *Geophysics, Geosystems*, 21, e2019GC008756. doi:10.1029/2019GC008756.
- 343 McEwen, A. S., Keszthelyi, L., Spencer, J. R., Schubert, G., Matson, D. L., Lopes-Gautier, R. M. C.,
- 344 Klaasen, K. P., Johnson, T. V., Head, J. W., Geissler, P., Fagents, S., Davies, A. G., Carr, M. H.,

- 345 Breneman, H. H., & Belton, M. J. S. (1998), High-temperature silicate volcanism on Jupiter's moon
346 Io. *Science*, 281, 87–90. doi:10.1126/science.281.5373.87.
- 347 McEwen, A. S., Belton, M. J. S., Breneman, H. H., Fagents, S. A., Geissler, P., Greeley, R., Head, J.
348 W., Hoppa, G., Jaeger, W. L., Johnson, T. V., Keszthelyi, L., Klaasen, K. P., Lopes-Gautier, R. M.
349 C., Magee, K. P., Milazzo, M. P., Moore, J. M., Pappalardo, R. T., Phillips, C. B., Radebaugh, J.,
350 Schubert, G., Schuster, P., Simonelli, D. P., Sullivan, R., Thomas, P. C., Turtle, E. P., & Williams,
351 D. A. (2000), Galileo at Io: Results from High-Resolution Imaging. *Science*, 288, 1193–1198.
352 doi:10.1126/science.288.5469.1193.
- 353 McEwen, A. S., et al. (2020), Tidal heating: Lessons from Io and the Jovian system; Relevance to
354 exoplanets. *Exoplanets in our Backyard, I*, abstract 3005.
- 355 McGovern, P. J., Kirchoff, M. R., White, O. L., & Schenk, P. M. (2016), Magma ascent pathways
356 associated with large mountains on Io. *Icarus*, 272, 246–257. doi:10.1016/j.icarus.2016.02.035.
- 357 McKinnon, W. B., Schenk, P. M., & Dombard, A. J. (2001), Chaos on Io: A model for formation of
358 mountain blocks by crustal heating, melting, and tilting. *Geology*, 29, 103–106. doi:10.1130/0091-
359 7613(2001)029<0103:COIAMF>2.0.CO;2.
- 360 Nahm, A. L., & Schultz, R. A. (2010), Evaluation of the orogenic belt hypothesis for the formation of
361 the Thaumasia Highlands, Mars. *Journal of Geophysical Research*, 115, E04008.
362 doi:10.1029/2009JE003327.
- 363 Peale, S. J., Cassen, P., & Reynolds, R. T. (1979), Melting of Io by tidal dissipation. *Science*, 203, 892–
364 894. doi:10.1126/science.203.4383.892.
- 365 Radebaugh, J., Keszthelyi, L. P., McEwan, A. S., Turtle, E. P., Jaeger, W. L., and Milazzo, M. (2001),
366 Paterae on Io: A new type of volcanic caldera? *Journal of Geophysical Research*, 106, 33,005–
367 33,020. doi:10.1029/2000JE001406.

- 368 Reches, Z. (1978), Development of monoclines: Part I. Structure of the Palisades Creek branch of the
369 East Kaibab monocline, Grand Canyon, Arizona. *Geological Society of America, Memoir 151*, 235–
370 271. doi:10.1130/MEM151-p235.
- 371 Riley, C. M., Diehl, J. F., Kirschvink, J. L., & Ripperdan, R. L. (1999), paleomagnetic constraints on
372 fault motion in the Hilina Fault System, south flank of Kilauea Volcano, Hawaii. *Journal of*
373 *Geophysical Research*, 94, 233–249. doi:10.1016/S0377-0273(99)00105-5.
- 374 Schenk, P. M., & Bulmer, M. H. (1998), Origin of mountains on Io by thrust faulting and large-scale
375 mass movements. *Science*, 279, 1514–1517. doi:10.1126/science.279.5356.1514.
- 376 Schenk, P. M., Hargitai, H., Wilson, R., McEwan, A., & Thomas, P. C. (2001), The mountains of Io:
377 Global and geological perspectives from Voyager and Galileo. *Journal of Geophysical Research*,
378 106, 33,201–33,222. doi:10.1029/2000JE001408.
- 379 Strom, R. G., Trask N. J., & Guest J. E. (1975), Tectonism and volcanism on Mercury. *Journal of*
380 *Geophysical Research*, 80, 2478–2507. doi:10.1029/JB080i017p02478.
- 381 Thaller, T. F. (2000), Galileo orbital operations Solid State Imaging raw EDR v1.0 [Data set]. NASA
382 Planetary Data System. doi:10.17189/1520425.
- 383 Turtle, E. P., Jaeger, W. L., Keszthelyi, L. P., McEwan, A. S., Milazzo, M., Moore, J., Phillips, C. B.,
384 Radebaugh, J., Simonelli, D., Chuang, F., Schuster, P., & the Galileo SSI Team (2001), Mountains
385 on Io: High-resolution Galileo observations, initial interpretations, and formation models. *Journal of*
386 *Geophysical Research*, 106, 33,175–33,199. doi:10.1029/2000JE001354.
- 387 Walter, T. R., & Troll, V. R. (2001), Formation of caldera periphery faults: an experimental study.
388 *Bulletin of Volcanology*, 63, 191–203. doi:10.1007/s004450100135.
- 389 Williams, D. A., Radebaugh, J., Keszthelyi, L. P., McEwen, A. S., Lopes, R. M. C., Douté, S., &
390 Greeley, R. (2002), Geologic mapping of the Chaac-Camaxtli region of Io from Galileo imaging
391 data. *Journal of Geophysical Research*, 107, E9, 5068. doi:10.1029/2001JE001821.

392 Williams, D. A., Keszthelyi, L. P., Crown, D. A., Yff, J. A., Jaeger, W. L., Schenk, P. M., Geissler, P.
393 E., & Becker, T. L. (2011), Geologic map of Io: U.S. Geological Survey Scientific Investigations
394 Map 3168, scale 1:15,000,000, 25 p., available at <https://pubs.usgs.gov/sim/3168/>.

395 **Figures**

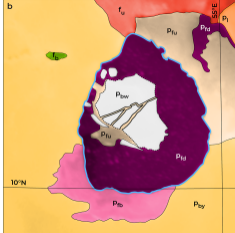
396 **Figure 1.** Loki Patera. (a) Combined monochrome Voyager 1 and color Galileo imagery at 1 km/pixel.
 397 The floor of the patera is dark, in contrast to the brighter polygonal island. We infer the dark, linear
 398 features crossing the island (green arrows) as extensional tectonic structures. Smaller patches of bright
 399 material dot the patera floor (blue arrows). The location of Loki Patera is shown with a purple diamond
 400 on the global Io mosaic (in Robinson projection). (b) A structural sketch of (a); the patera and main
 401 island are outlined in a solid blue and dotted black lines, respectively. The boundaries of the features
 402 we interpret to be extensional structures are shown with solid black lines. The units shown are from the
 403 Io global geological map (Williams et al., 2011). This scene is in azimuthal equidistant projection,
 404 centered at 13.2°N, 51.3°E.

406 **Figure 2.** A portion of Emakong Patera, which has straight edges (green arrows) that terminate at sharp
 407 corners (Radebaugh et al., 2001). The location of Emakong Patera is shown on the global Io mosaic.
 408 The main scene comprises Galileo SSI images 5000r, 5139r, and 5140r, and is in azimuthal equidistant
 409 projection, centered at 3.5°S, 240.0°E.

411 **Figure 3.** Hi'iaka Montes, examples of thrust fault-bounded mountain blocks on Io that show
 412 substantial evidence for extensional deformation (pink arrows). The blue arrow indicates a lava flow.
 413 The position of Hi'iaka Montes is shown on the global Io mosaic. The main scene comprises Galileo
 414 SSI images 7465r, 7478r, and 7500r, and is in azimuthal equidistant projection, centered at 4.5°S,
 415 279.0°E.

417 **Figure 4.** A schematic showing thrust faults (heavy black lines) dominating the lower part and
 418 extensional structures (thin black lines) throughout the upper part of Io's lithosphere. Example
 419 kinematic indicators are shown, as are magma bodies (examples marked by white arrows) and where

420 magma is ascending along normal faults (yellow arrows). The principal compressive stresses for the
421 upper and lower lithosphere are also shown; σ_H and σ_h are horizontal stresses, and σ_v is the vertical
422 stress. Where mountains are present, deep-seated thrusts extend to the surface (not shown here).



UNITS

from Williams et al. (2011)

	P_{bw}	white bright plains material
	P_{by}	yellow bright plains material
	P_{fb}	bright patera floor material
	P_{fd}	dark patera floor material
	P_{fu}	undivided patera floor material
	f_b	bright flow material
	f_u	undivided flow material
	P_l	layered plains material

	patera outline
	patera island outline
	extensional structure

Notes: Units are not shown here in stratigraphic order.

